Bulk quantities in nuclear collisions from running-coupling k_T factorization and hybrid simulations

Andre V. Giannini,[1,2] Frédérique Grassi,[2] and Matthew Luzum[2]
[1]*Akita International University, Yuwa, Akita 010-1292, Japan*
[2]*Instituto de Física, Universidade de São Paulo, Rua do Matão 1371, 05508-090 São Paulo, São Paulo, Brazil*

(Received 9 May 2019; published 31 July 2019)

Starting from a color glass condensate (CGC) framework, based on a running-coupling improved k_T-factorized formula, we calculate bulk observables in several heavy-ion collision systems. This is done in two ways: first we calculate the particle distribution directly implied from the CGC model, and we compare this to the case where it is instead used as the initial condition for a hybrid hydrodynamic simulation. In this way, we can assess the effects of hydrodynamic and hadronic evolution by quantifying how much they change the results from a pure initial state approach and, therefore, to what extent initial condition models can be directly compared to experimental data. We find that entropy production in subsequent hydrodynamic evolution can increase multiplicity by as much as 50%. However, disregarding a single overall normalization factor, the centrality, energy, and system size dependencies of charged hadron multiplicity are only affected at the ∼5% level. Because of this, the parameter-free prediction for these dependencies gives reasonable agreement with experimental data whether or not hydrodynamic evolution is included. On the other hand, our model results are not compatible with the hypothesis that hydrodynamic evolution is present in large systems, but not in small systems like p-Pb, in which case the dependence of multiplicity on system size would be stronger than seen experimentally. Moreover, we find that hydrodynamic evolution significantly changes the distribution of momentum, so that observables such as the mean transverse momentum are very different from the initial particle production and much closer to measured data. Finally, we find that a good agreement to anisotropic flow data cannot be achieved due to the large eccentricity generated by this model.

DOI: 10.1103/PhysRevC.100.014912

I. INTRODUCTION

Current colliders operating at ultrarelativistic energies—the BNL relativistic Heavy Ion Collider (RHIC) and the CERN Large Hadron Collider (LHC)—are designed to study the behavior of nuclear matter under extreme conditions. The matter formed right after a high-energy collision is thought to be a system out of equilibrium with a large gluon occupation number, so each gluon carries a small fraction of momentum, $x \ll 1$, of the original hadron [1]. This implies that the knowledge of the properties of the small-x modes of the hadronic wave function is very important to understanding the initial stages of hadronic collisions at high energies. Over the years much effort has been devoted to doing so, and it is now well established theoretically that such properties can be described in terms of the color glass condensate (CGC) effective-field theory [1–3]. Among other important features, the CGC encodes nonlinear dynamics and effects of the parton saturation[1] phenomena, which restore the unitarity of the scattering matrix and are characterized by a dynamical scale Q_s, the saturation scale, considered to be the typical momentum scale in the hadronic wave function. The presence of this scale, which increases with the energy of the collision and the atomic number, allows one to treat particle production on a solid basis where perturbative methods can be applied.

After the initial particle production, the system can continue to interact and evolve. In collisions between heavy nuclei (and possibly in smaller systems [5–15]), after a short period of time $\tau < 1$ fm/c, the system is believed to behave as a relativistic fluid. Indeed, viscous hydrodynamic simulations have been quite successful at describing and predicting various experimental data [16–31].

Particle number is intimately related to entropy, and in the limit of ideal hydrodynamics (i.e., zero viscosity), entropy is conserved during the evolution of the system. Dissipative effects (from viscous evolution as well as any nonhydrodynamic process such as the later decay of resonances) break this conservation. Nevertheless, because of this expected approximate entropy conservation, it is common to directly compare particle distributions in the initial state with experimental data on bulk quantities like total multiplicity and its dependence on rapidity, centrality, collision energy, and the collision system. This allows one to quickly gauge the success of theoretical models of particle production, under the assumption that subsequent evolution of the system will not change these bulk quantities.

[1]The saturation of the partonic density inside a hadron is a direct consequence of the well-known steep increase of the gluon density with lowering x [3,4] that is driven by the gluon emission process, $g \to gg$. In simple terms, it can be understood as the inclusion of the gluon recombination process ($gg \to g$), which starts to be non-negligible due to the high density of gluons in the hadronic wave function.

There exist comparisons between CGC and hydrodynamics calculations, with both sharing the same initial state dynamics [32–34]. However, the comparisons are limited, for example, involving only a single collision system and energy.

In this work we compute global, bulk observables obtained separately from a purely CGC model, and a hybrid (hydro + transport) model simulation that shares the same initial state dynamics. Such a procedure allows us to assess the effects of hydrodynamic and hadronic evolution and quantify to what extent initial condition models can be directly compared to experimental data. Different from previous studies we compare the results of both simulations for different energies, from RHIC to LHC, and collision systems, including predictions for O + O and Ar + Ar that may be part of the LHC program in the future [35]. In the next section we briefly present the ingredients of each simulation and then the results following from each one of them.

II. CGC AND HYBRID SIMULATIONS

In the dilute-dense approximation, a k_T-factorized expression for inclusive small-x gluon production in the scattering of two valence quarks can be derived [36]. This approximation is natural for asymmetric collisions such as p-A. Conversely, the applicability to symmetric $A + A$ collisions at midrapidity is not clear. In the latter case, due to its increasing complexity, one expects factorization-breaking corrections that modify the basic k_T-factorized expression. Although such corrections have already been studied [37] in the past, the magnitude of these corrections in the kinematical range probed at the LHC is still unknown.

On the other hand, while the correct momentum distribution in $A + A$ collisions can still only be reliably obtained by means of "dense-dense" calculations, which make no use of such k_T-factorized formula [38], phenomenological applications of the k_T-factorized expression [39–43] have been able to correctly describe the centrality and energy dependence of the charged hadron multiplicity. This can be understood as an indication that, for large nuclei and high energies, these observables are mainly determined by the centrality and energy dependence of the saturation scale and might not be highly affected by factorization-breaking effects. Following the success of previous works, we also apply a k_T-factorized expression to obtain momentum-integrated quantities in $A + A$ collisions.

Originally, such a k_T-factorized expression was derived in a fixed-coupling approximation [36]. Corrections related to the running of the QCD coupling were calculated in Ref. [44]. While the initial result was obtained for a fixed-rapidity configuration, the authors proposed the following generalization of how these running-coupling corrections would modify the leading-order expression in the presence of nonlinear small-x evolution:[2]

$$\frac{d\sigma}{dyd^2kd^2b} = N\frac{2C_F}{\pi^2}\frac{1}{\boldsymbol{k}^2}\int d^2q \int d^2b' \overline{\phi}_{h_1}(\boldsymbol{q}, x_1, \boldsymbol{b}')\overline{\phi}_{h_2}(\boldsymbol{k}-\boldsymbol{q}, x_2, \boldsymbol{b}'-\boldsymbol{b})\frac{\alpha_s\left(\Lambda^2_{\rm coll}e^{-5/3}\right)}{\alpha_s(Q^2e^{-5/3})\alpha_s(Q^{*2}e^{-5/3})}, \tag{1}$$

where N is an overall normalization to be fixed by comparison with the experimental data; $C_F = (N_c^2 - 1)/2N_c$, with $N_c = 3$; $x_{1,2} = (k_T/\sqrt{s})\exp(\pm y)$ is the momentum fraction of the projectile and the target quark, respectively; and $\Lambda^2_{\rm coll}$ is a collinear infrared cutoff. Despite including higher-order corrections, note that Eq. (1) is still k_T factorized. The number of produced gluons with rapidity y and momentum k at a coordinate $\boldsymbol{b}$ in the transverse grid in a given hadronic collision $h_1 + h_2$ can be obtained from Eq. (1) as

$$\frac{dN_g}{dyd^2kd^2b} = \frac{1}{\sigma_s}\frac{d\sigma}{dyd^2kd^2b}, \tag{2}$$

with σ_s representing the effective interaction area of the hadrons h_1 and h_2.

In the above equation, $\overline{\phi}_{h_i}(\boldsymbol{k}, x, \boldsymbol{b})$ denotes the unintegrated gluon distribution (UGD), which represents the probability of finding a gluon with momentum fraction x with transverse momentum k_T in the hadron h_i [45]. This distribution can be expressed as [44]

$$\overline{\phi}(\boldsymbol{k}, y, \boldsymbol{b}) = \alpha_s\phi(\boldsymbol{k}, y, \boldsymbol{b}) = \frac{C_F}{(2\pi)^3}\int d^2r e^{-i\boldsymbol{k}\cdot\boldsymbol{r}}\,\nabla_r^2\mathcal{N}_A(\boldsymbol{r}, y, \boldsymbol{b}), \tag{3}$$

with $\mathcal{N}_A(\boldsymbol{r}, y, \boldsymbol{b})$ denoting the forward dipole scattering amplitude in the adjoint representation at impact parameter $\boldsymbol{b}$. Although some advances have been made very recently [46], computing the matter distribution in the $\boldsymbol{b}$ space inside a proton directly from the CGC framework is still an open and nontrivial problem [47]. Due to this limitation, a uniform gluon density within the proton has been assumed; in this case, the integration over d^2b' in Eq. (1) generates a factor proportional to σ_s that cancels out with the same factor in the denominator of Eq. (2). Moreover, $\mathcal{N}_A$ will be given by solutions of the running-coupling Balitsky-Kovchegov (rcBK) equation [48] provided by the AAMQS fit of the HERA data on lepton-hadron collisions [49]. Here we consider their solution with the McLerran-Venugopalan model [49] as the initial condition. We note, however, that results for bulk observables do not differ much when considering other UGD sets that employ different initial conditions for the rcBK evolution [50].

Apart from incorporating running coupling corrections, the other novel feature of Eq. (1) is the fact that all the scales present in the α_s factors are fixed and determined by explicit

[2]The notation follows the one from Ref. [44]: $\boldsymbol{k}$ denotes the transverse momentum of the produced gluon, while $\boldsymbol{q}$ and $\boldsymbol{k} - \boldsymbol{q}$ are the "intrinsic" transverse momenta from the gluon distributions.

calculations.[3] We refer to Ref. [44] for the full expression of the Q^2 dependence for the two α_s factors appearing explicitly in Eq. (1). A comparison of the centrality dependence of charged hadron multiplicity in $p+\mathrm{Pb}$ and $\mathrm{Pb}+\mathrm{Pb}$ collisions [43] has shown a difference of $\sim$10% in the results from Eq. (1) and the fixed-coupling k_T-factorization formula with the momentum scales figuring in the α_s factors fixed by hand.

Equation (1) is the starting point for each calculation. In the case where hydrodynamic evolution is absent, one must still convert this spectrum of gluons into that of the hadrons that are measured. This can be done by a convolution with a fragmentation function that represents the hadronization process. By doing so, one also fixes $\Lambda^2_{\mathrm{coll}}$, because it should match the momentum scale figuring in the fragmentation function [51] (which is usually chosen to be proportional to the transverse momentum of the produced hadron, $\mu^2_{\mathrm{FF}} \sim p_T^2$). While Eq. (1) implicitly assumes the validity of collinear fragmentation functions to convert gluons into hadrons [44,51], these ingredients have important limitations on their range of applicability, being restricted to large momenta, usually above 1 GeV. Because bulk observables, like the ones we are interested in here, have significant contribution below this regime, they miss most of the dynamics encoded in these fragmentation functions. Because of this, we use the local parton-hadron duality (LPHD) [52] as the fragmentation model, where distributions at partonic and hadronic levels only change by a constant multiplicative factor.

This same setup has already been considered in Refs. [53] and [43] where Eq. (1) has been employed to obtain, respectively, qualitative and quantitative results for bulk observables in the CGC approach. Here, the pure CGC simulation follows the one of Ref. [43], which we extend to the calculations of the average transverse momentum. Moreover, we present predictions for the centrality dependence of the charged hadron multiplicity that may be measured in other collision systems ($\mathrm{Ar}+\mathrm{Ar}$ and $\mathrm{O}+\mathrm{O}$) that were not considered before in those pure CGC works.[4] The use of the LPHD is equivalent to disregarding any medium or dynamical effects during the evolution of the system created after the collision or after the transition from a state of deconfined matter to hadrons. This approximation will be contrasted to the results from a more complete simulation of heavy-ion collisions where such medium effects and the dynamics at the hadronic level are accounted for.

In the case where collisions are described via a hybrid model, the initial conditions for hydrodynamic evolution consist of the energy momentum tensor $T^{\mu\nu}$ at some initial time. Because we are mainly interested in midrapidity observables, we perform boost-invariant simulations, with initial conditions based on the distribution of gluons at zero rapidity. Specifically, we take the entropy density to be proportional to the gluon density from the CGC framework

$$s(\boldsymbol{b}, \tau = \tau_0) \propto \left.\frac{dN_g}{d^2b dy}\right|_{y=0}, \tag{4}$$

where the $dN_g/d^2b dy$ can be obtained by integrating Eq. (2) over d^2k. The corresponding energy density is then obtained by thermodynamic relations from an equation of state derived from lattice QCD calculations, s95p-v1.2 [57]. We assume zero initial shear tensor and bulk pressure, and no initial transverse fluid velocity.

In the above expression, τ_0 represents the time at which the system starts behaving hydrodynamically. Because we do not include any pre-equilibrium description of the system and also only account for the diagonal terms of the energy-momentum tensor, we assume that early and or fast thermalization happens so the produced system can start expanding in all directions as it should. The results presented in the next section have been obtained using $\tau_0 = 0.2$ fm; the proportionality constant figuring in $s_0(\boldsymbol{b})$ is fixed through the same experimental data used to fix the overall normalization in the pure CGC simulation.

Here we consider the cases where the system evolves hydrodynamically with and without the presence of dissipative corrections in $T^{\mu\nu}$. The resulting equations of motion in the dissipative case are the ones from the second-order viscous hydrodynamics presented in Ref. [58]. Those are solved using the MUSIC code [59]. The cessation of hydrodynamic evolution is described by switching to the hadronic afterburner UrQMD [60] once the system has locally reached the chosen switching temperature T_{sw}.

We choose hydrodynamic parameters $[\eta/s(T),\ \zeta/s(T),\ T_{\mathrm{sw}}]$ to correspond to the maximum *a posteriori* parameters from a comprehensive Bayesian analysis [61].[5] That analysis used different initial conditions, and therefore these parameters are not necessarily the choices that will give the best fit to experimental data for our initial conditions. Nevertheless, they represent a reasonable and realistic starting point.

The effects of dissipation are estimated by completing a separate set of ideal hydrodynamic simulations, with exactly the same set of initial conditions.

As seen above, the CGC is a natural choice of initial conditions. Therefore we compare two different scenarios: the pure CGC and the hybrid simulations (with CGC initial conditions). Because both simulations have a common starting point, it allows for a more consistent comparison.

In the next section we compare our results for the centrality and energy dependencies of charged hadrons produced in heavy-ion[6] and $p+A$ collisions at RHIC and LHC energies from the pure CGC (denoted as rcBK) and from the hybrid model (with ideal or viscous hydrodynamics evolution; each

[3] In contrast, in the fixed-coupling expression, the α_s factors in the denominator of Eq. (1) are part of the UGD definition, given by the first equality in Eq. (3), and have to be fixed by hand.

[4] However, see Refs. [54–56] for hydrodynamic-based calculations.

[5] Reference [61] presents the results of several analyses. The values considered here are the ones quoted in Table 5.8, corresponding to the most recent.

[6] The isotope ^{229}Xe has been used for collisions involving xenon nuclei at LHC energies; the parameters characterizing its deformation are the same as those from Table II of Ref. [62].

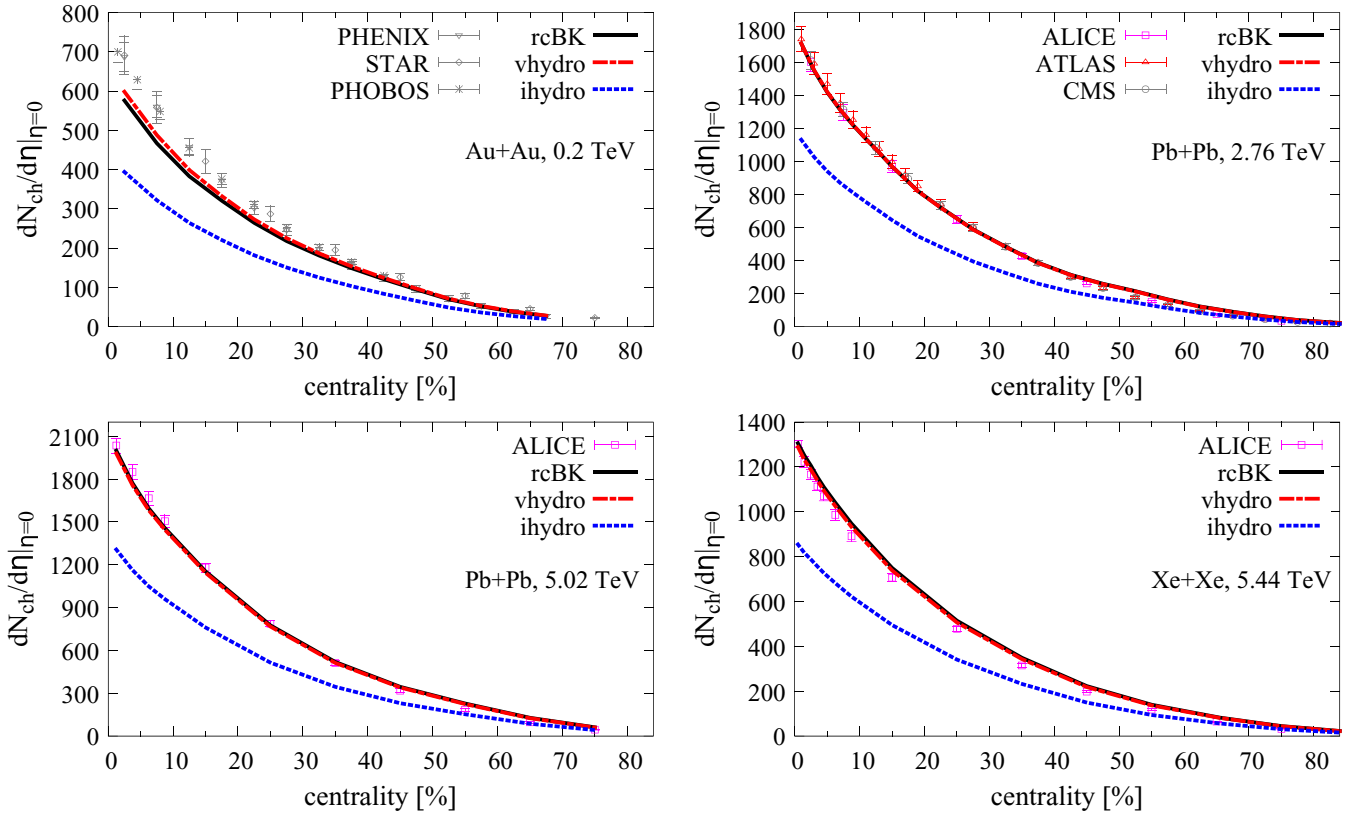

FIG. 1. Centrality dependence of charged hadron multiplicity in the central pseudorapidity region produced in $A + A$ collisions at RHIC and LHC energies. The experimental data are from Refs. [63–69].

case is simply denoted by ihydro and vhydro, respectively) simulations.

III. RESULTS AND DISCUSSION

Figure 1 shows the centrality dependence of the charged hadron multiplicity produced in the central pseudorapidity region of $A + A$ collisions at RHIC top energy and also at different LHC energies. The normalization has been fixed by matching the rcBK and the vhydro results to the data for central Pb + Pb collisions at 2.76 TeV. The normalization of the viscous hydrodynamic (vhydro) results has also been applied to the ideal hydrodynamic (ihydro) ones. The same normalization is used across all energies and collision systems.

We see that the pure CGC calculation gives a reasonable, but not perfect, fit to the data. The hybrid calculation gives similar results, showing that, indeed, the dynamics of the late stages of nuclear collisions have only a small effect on how the multiplicity of charged hadrons is distributed across centrality, energy, and collision systems. Moreover, the poorest fit to data occurs at the lowest collision energies.

We also present predictions from the pure CGC and hybrid simulations for the centrality dependence of the charged hadron multiplicity produced in Ar + Ar and O + O collisions (as proposed for the LHC) in Fig. 2. While our rcBK and vhydro results for Ar + Ar collisions are similar to the ones presented in Ref. [55] (which use a different initial condition for their hydrodynamic calculation), their results are about 30% higher than ours for central O + O collisions.

In Fig. 3 we show the energy evolution of the charged hadron multiplicity per participant (pair) in $p + A$ $(A + A)$ collisions from the present hybrid simulation and the rcBK results. We can see that in $A + A$ collisions, the pure CGC model predicts an energy dependence stronger than that seen in experimental data. Including hydrodynamic evolution counteracts this by weakening the energy dependence, but the

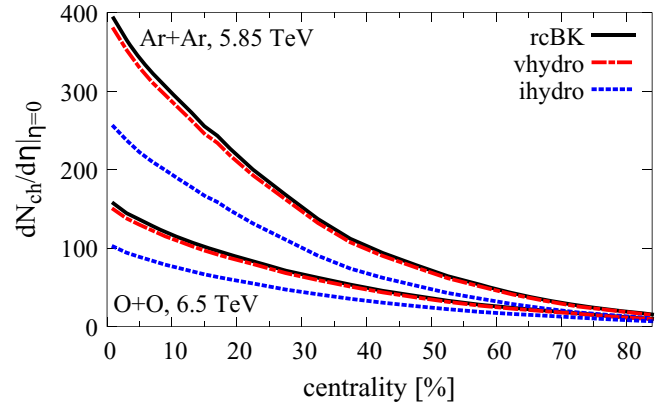

FIG. 2. Prediction for the centrality dependence of the charged hadron multiplicity produced in Ar + Ar and O + O collisions.

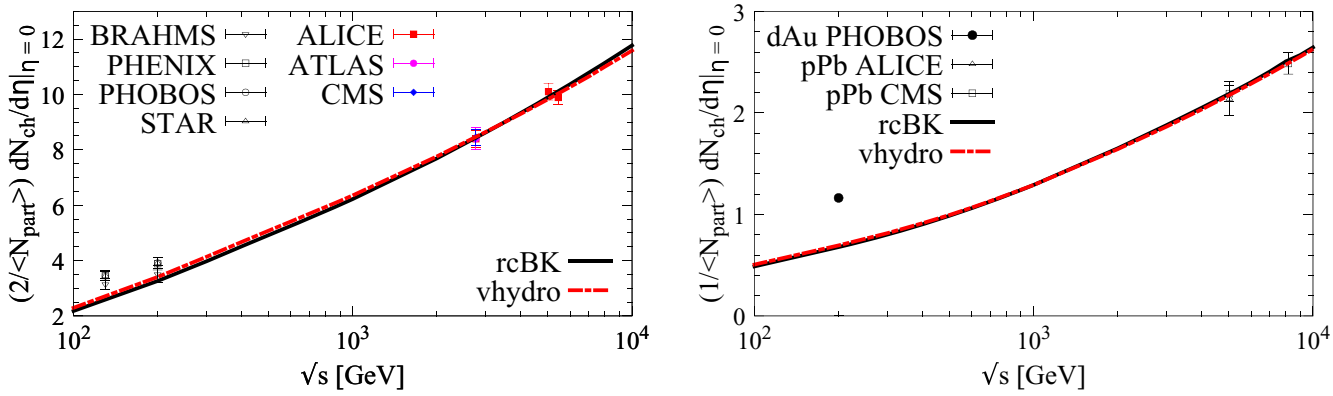

FIG. 3. Energy dependence of the charged hadron multiplicity in (left) 6% most central $A + A$ collisions and (right) minimum-bias $p + \mathrm{Pb}$ collisions. The experimental data are from Refs. [63–72].

effect is too small to achieve agreement with experimental data.

Similarly, the predicted energy dependence in light-heavy systems also appears to be too strong. Note that the calculation presented in the right panel of Fig. 3 is for $p + \mathrm{Pb}$ collisions, while the lowest-energy experimental point is for a d-Au system. However, we checked that there is no improvement at 200 GeV if we consider $d + \mathrm{Au}$ collisions instead.

Improving the rcBK results (and therefore the corresponding initial condition for hydro simulations) at RHIC energies for $p(d) + A$ collisions requires a better knowledge of the proton unintegrated gluon distribution at $x \sim 0.1$. This will certainly have an impact on the results for $A + A$ collisions in the same energy range because nuclear distributions are usually built from what is known about the proton's structure function. Such improvement will be possible in the future because our knowledge about (un)integrated parton distribution functions will be improved with the help of an (so far planned) electron-ion collider.

We can better quantify the effect of final-state evolution by calculating ratios of charged hadron multiplicity in CGC compared to hybrid calculations. In Fig. 4, multiplicity ratios are presented as a function of centrality in $A + A$ and center-of-mass energy in $p + A$ and $A + A$ collisions. On the left, one can see that the ratio is almost constant as a function of centrality, showing no more than a few percent change. The largest differences come with a change in collision energy and colliding system. Recall that the normalization factor was set from central $\mathrm{Pb} + \mathrm{Pb}$ collisions at 2.76 TeV. The biggest difference in multiplicity comes in the system with the largest difference in energy—$\mathrm{Au} + \mathrm{Au}$ at 0.2 TeV, where the vhydro multiplicity is ∼5% higher than rcBK.

The dependence on energy of the multiplicity ratio is shown explicitly in the right panel of Fig. 4 for the 6% most central Pb-Pb collisions as well as for p-Pb collisions. Across 2 orders of magnitude in collision energy, hydro and final state effects change the predicted multiplicity by slightly more than 6% for the $A + A$ system and 4.5% for the $p + A$ system.

While most of the total entropy produced in a collision typically comes from its initial stage, a significant amount can potentially be produced during hydrodynamic evolution, which in turn causes an increase in the charged hadron multiplicity.

As entropy is exactly conserved in ideal hydrodynamics, a ratio of the final hadron multiplicity generated assuming ideal and viscous hydrodynamics evolution can be used as a proxy to quantify the entropy which is produced on top of the initial one after the particles that compose such a system

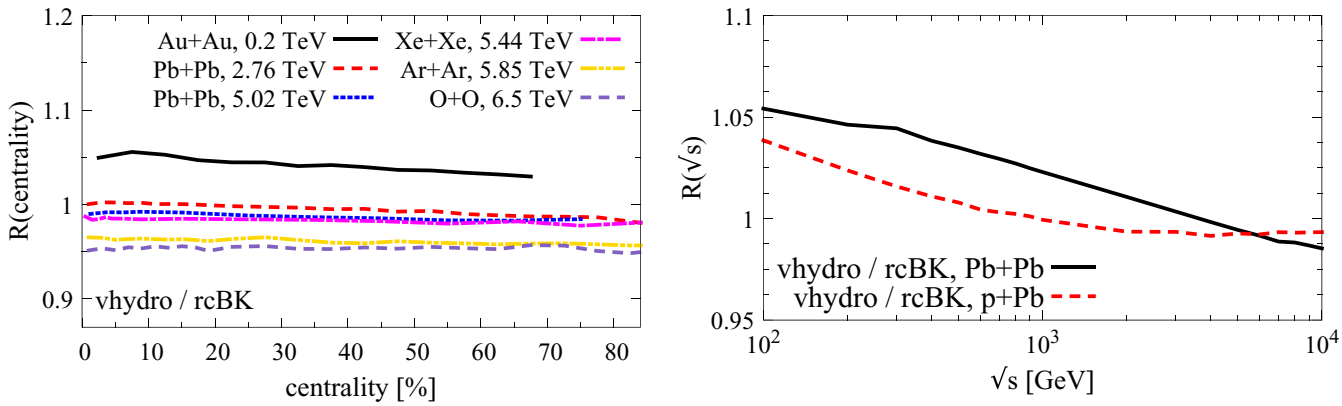

FIG. 4. Centrality and energy dependencies of the ratio of our results with viscous hydrodynamics to the ones with only initial state dynamics for the charged hadron multiplicities.

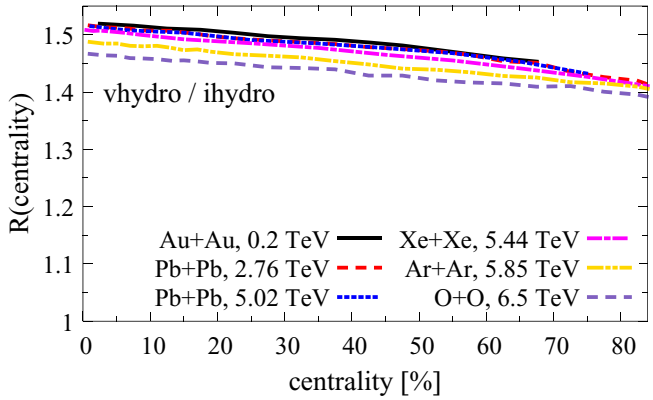

FIG. 5. Centrality dependence of the ratio of our results with viscous and ideal hydrodynamics for the charged hadron multiplicity and its transverse energy distribution for selected collision systems.

stop interacting inelastically. Figure 5 shows the centrality dependence of such a ratio for several collision systems and energies. As one can see, up to ∼50% of the final multiplicity is produced from dissipative effects happening during the late stages for the 0–10% most-central heavy-ion collisions in the $0.2\ \text{TeV} \leqslant \sqrt{s} \leqslant 5.44\ \text{TeV}$ region; for intermediate collision systems such as Ar + Ar and O + O, almost as much extra entropy is produced from hydro and final state effects in this same centrality range. Although smaller systems might have a larger rate of entropy production, in this case, their shorter lifetime (at similar energies) ensures that less total entropy is produced. The production of entropy decreases quite slowly for nonperipheral collisions and even collisions happening at 40% of the centrality range have between ∼49%–42% of the final multiplicity from hydro and final state effects (the first value is for Au + Au and the second one is for O + O).

This hydrodynamic entropy production leads to an interesting observation: while we are able to describe the data for global, bulk observables in both heavy-ion and light-ion collision systems when hydrodynamic evolution is either present or absent in both systems, our results are incompatible with the case where it is included in $A + A$ collisions, but there is no hydrodynamic evolution in $p + A$ collisions, as has been suggested [73–75]. In that scenario there would be a decrease in the overall magnitude of charged hadron multiplicity in smaller systems due to the absence of viscous entropy production.

Next we consider the distribution of momentum and how it is affected by hydrodynamic evolution. Figure 6 shows our results for the centrality dependence of the average transverse momentum of charged hadrons at mid-pseudorapidity in heavy-ion collisions at RHIC[7] and LHC energies and p + Pb collisions also in the LHC regime. The measurement has not been performed in p + Pb collisions as a function of centrality or multiplicity, so we show the minimum-bias result [77] as a gray band in the bottom right panel of Fig. 6.

The rcBK results are significantly larger and show a faster increase with the centrality of the collision with respect to the experimental data. Such a feature can be related to the increase of the saturation scale, $Q^2_{s,\text{nucl}} \sim N_{\text{part}}\, Q^2_{s,\text{proton}}$, together with an effective "free-streaming" space-time evolution of the system leading to a final energy distribution per particle that is close to the initial one.

Unlike the case of multiplicity, whose centrality dependence is little changed by hydrodynamic evolution, the distribution of transverse momentum is more sensitive to the dynamics happening during the evolution of the system [79–81]. This fact is illustrated by the vhydro results, which show a slower increase of $\langle p_T \rangle$ with centrality and are much closer to the experimental data.

It has been argued [31] that the ratio of mean transverse momentum in systems of different size but at the same energy gives a robust test of hydrodynamic behavior. That is, it should depend little on the details of a hydrodynamic system, but could be quite different for a system with different dynamics. To illustrate this, we show in Fig. 7 (left panel) the ratio of the average transverse momentum in Xe + Xe and Pb + Pb collisions at 5.44 and 5.02 TeV, respectively.

The scale invariance of ideal hydrodynamics predicts that $\langle p_T \rangle$ should not change with system size, broken only by dissipative corrections.

Indeed, we see that our ideal hydrodynamic calculation gives a ratio that is close to 1, in agreement with the recent measurement from the ALICE Collaboration. Our viscous calculation is somewhat lower but is consistent within error bars up to ∼40% centrality. Both results have the same shape and differ by less than 2%, largely confirming the robustness of the hydrodynamic prediction, though perhaps indicating a potential probe of viscosity.

On the other hand, the pure initial state rcBK calculation is below the hydro prediction and clearly incompatible with measured data. We checked that this ratio decreases about 2%, moving it farther away from the data (and the results of the hybrid simulations), in case one considers the KLN UGD instead of the rcBK one. Because $\langle p_T \rangle \sim Q_{s,A}$ in the CGC framework and $Q^2_{s,A} \sim A^{1/3} Q^2_{s,\text{proton}}$ for nuclear targets (recall that $A^{1/3}$ is, roughly, the nuclear density probed by a projectile passing through the center of a nucleus of mass number A), the generic expectation would be $\langle p_T \rangle_{\text{XeXe}} / \langle p_T \rangle_{\text{PbPb}} \sim (129/208)^{1/6} \sim 0.92$, so that initial state models based on a k_T-factorized expression would undershoot the data for the ratio of the average transverse momentum in Xe + Xe and Pb + Pb collisions. This measurement then imposes an important constraint on comparing initial state models to observables involving the distribution of energy between produced particles because, even though much of the uncertainty related to the absolute value of the average transverse momentum is canceled when taking a ratio, the pure CGC calculation is still not in agreement with it in any centrality range.

We note that the split between each calculation (the pure initial state and the hybrid simulation with ideal and viscous hydrodynamics) becomes more apparent if one still keeps a

[7]The PHENIX data [76] at 200 GeV have originally been presented for identified particles (pions, protons, and kaons); in this case we loosely identify the sum of the average momentum of each particle species weighted by their relative fraction of the total particle multiplicity as a rough representation of the average transverse momentum of (unidentified) charged hadrons.

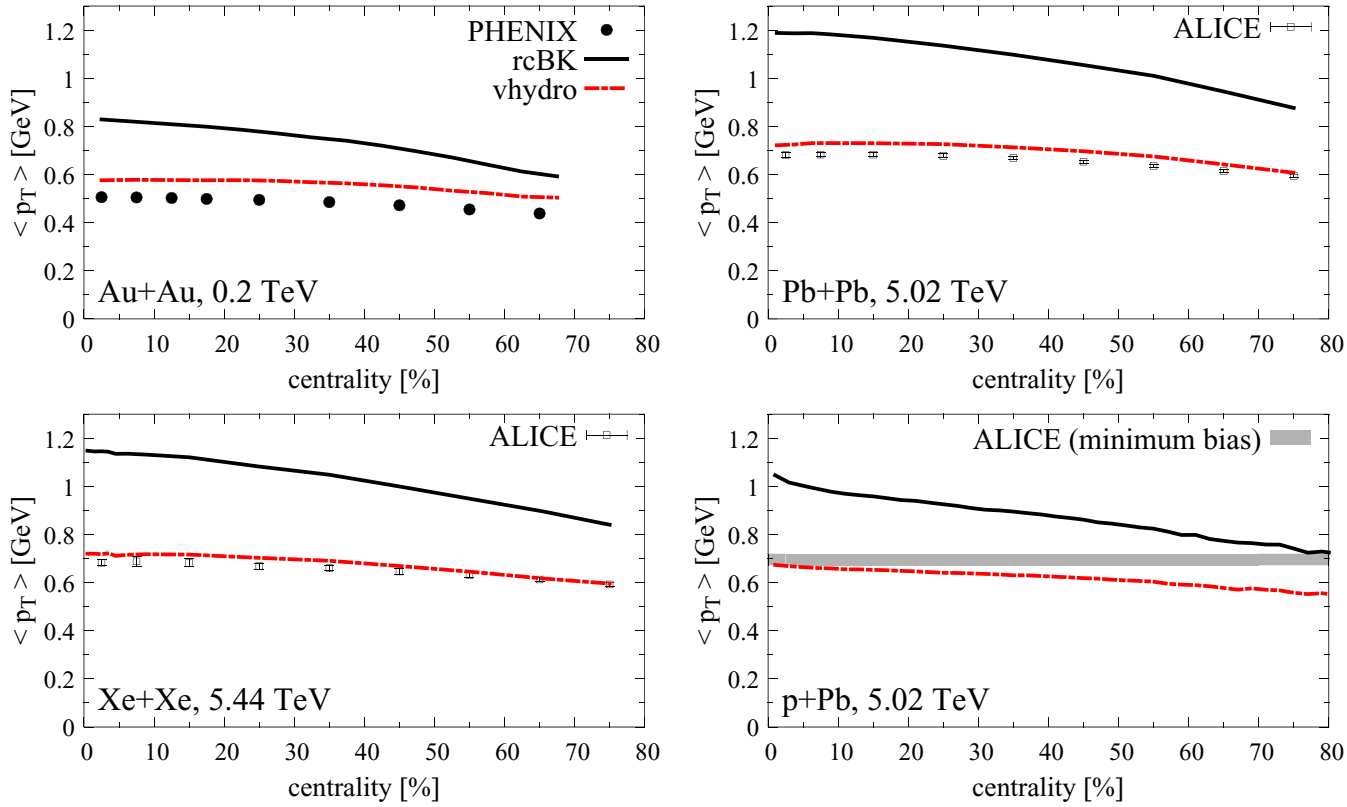

FIG. 6. Centrality dependence of the average transverse momentum of charged hadrons in Au + Au, Pb + Pb, Xe + Xe, and p + Pb collisions. The experimental data are from Refs. [76–78].

similar collision energy but increases the difference in system size with respect to Pb-Pb collisions. This is demonstrated in the right panel of Fig. 7, where now the average transverse momentum of charged hadrons produced in Ar-Ar collisions is compared to the same quantity in Pb-Pb collisions. This signals that the onset of a hydrodynamic phase in heavy-ion collisions, along with viscous effects, could, perhaps, be further investigated by studying the centrality dependence of ratio of the mean p_T across different collision systems with similar collision energies.

Last, in Fig. 8 we compare the results of our hybrid simulation to the centrality dependence of the integrated nth harmonic from two- and four-particle correlations, $v_n\{2\}$ and $v_n\{4\}$ from Pb + Pb collisions at LHC energies. Despite the satisfactory agreement between the hybrid simulation and the bulk observables studied so far, we find that the rcBK initial conditions from a running-coupling improved k_T-factorized expression still generate large eccentricities (on average), which in turn lead to angular asymmetries that are larger than the ones observed experimentally by the ALICE [82,83] Collaboration. Because our hybrid model overshoots $v_2\{2\}$ while being in agreement with $v_3\{2\}$, it would be impossible to get a simultaneous description of these harmonics for any value of viscosity with this initial condition. This is in line with

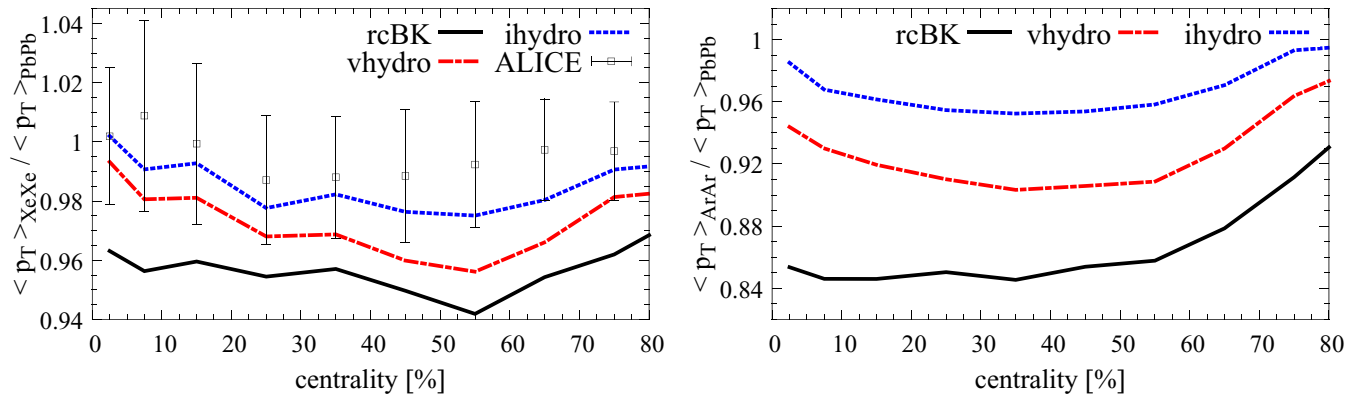

FIG. 7. Centrality dependence of the ratio of the transverse energy per charged particle from (left panel) Xe + Xe collisions at 5.44 TeV and Pb + Pb collisions at 5.02 TeV and (right panel) Ar + Ar collisions at 5.85 TeV and Pb + Pb collisions at 5.02 TeV.

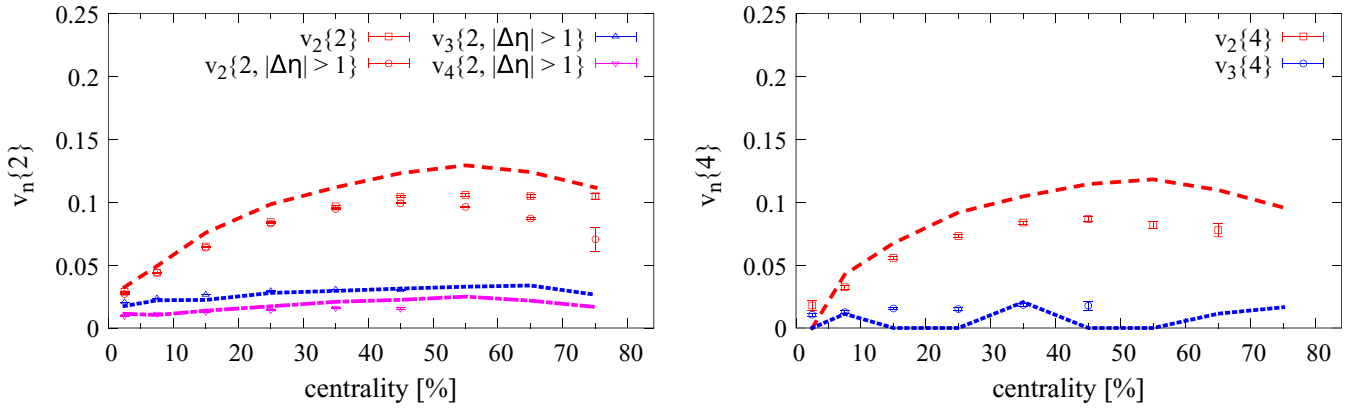

FIG. 8. Centrality dependence of $v_n\{2\}$ and $v_n\{4\}$ in Pb + Pb collisions at 2.76 TeV from the hybrid simulation. The experimental data are from Refs. [82,83].

previous studies that considered the leading-order version of Eq. (1) [84] where the running of the coupling has been fixed by hand, as well as with the previous k_T-factorized MC-KLN model [85–87]. In all these cases, the average eccentricity of the early-time system is larger than can be accommodated.

IV. CONCLUSIONS

In this work we calculated bulk observables measured in the central rapidity region at different collider energies from a CGC framework for particle production and from a hybrid model initialized by the same CGC calculation. Due to the use of local parton-hadron duality in this simulation, the rcBK dynamics represents all its dynamic content and determines the shape of observables. This approximation has been compared with a hybrid hydrodynamic simulation, which accounts for medium and final state effects, and which has been initialized using the same CGC dynamics so that both approaches have an intersecting point.

Assuming that fast thermalization occurs, we estimate that up to ∼50% of the final state multiplicity observed in heavy-ion collisions can come from dissipative effects during hydrodynamic evolution.

However, after fixing a single normalization factor in each of the two cases, we find that that the centrality dependence of the charged hadron multiplicity is insensitive to the late stage dynamics, matching the ones from the pure CGC simulation for different collision systems and collision energies in a wide centrality range. This fact is also seen in the energy evolution of the charged hadron multiplicity, where both simulations do not differ more than 5% in an energy range from 100 GeV to 10 TeV.

In contrast, the present framework does not accommodate the case where hydrodynamic evolution is present in $A + A$ collisions but not $p + A$ collisions. In that case, the entropy production in the large system can no longer be ignored as an overall constant factor, and the system size dependence of multiplicity would be significantly stronger than seen experimentally.

The evolution of the system and late stage dynamics do play an important role in redistributing momentum between the produced particles, resulting in a much better agreement with the measured average transverse momentum. We point out that comparing the average transverse momentum in Pb-Pb collisions to the same quantity in other colliding systems (at similar energies) as a function of centrality could be considered for two purposes: to investigate the onset of the hydrodynamical phase in high-energy heavy-ion collisions and to probe the effects of viscosity in different colliding systems.

Finally, we verified that the running-coupling corrections encoded in Eq. (1) do not change previous results for harmonic flow coefficients [84] where a leading-order expression with the running of the coupling fixed by hand was used, and that a large relative value $\varepsilon_2/\varepsilon_3$ prevents good agreement with measured data of elliptic and triangular flow.

ACKNOWLEDGMENTS

We thank Jorge Noronha for useful discussions, Marco van Leeuwen for information related to the ALICE data, and Jacquelyn Noronha-Hostler for comments on the draft. A.V.G. thanks Yu. Kovchegov for useful email exchange and acknowledges the Brazilian funding agency FAPESP for financial support through Grants No. 2017/14974-8 and No. 2018/23677-0. F.G. acknowledges support from Conselho Nacional de Desenvolvimento Científico e Tecnológico (CNPq, Grant No. 310141/2016-8). M.L. acknowledges support from FAPESP (Projects No. 2016/24029-6 and No. 2017/05685-2). F.G. and M.L. acknowledge support from project INCT-FNA (Grant No. 464898/2014-5). A.V.G. acknowledges the use of the resources of High Performance Computing made available by the Superintendência de Tecnologia da Informação da Universidade de São Paulo.

[1] E. Iancu and R. Venugopalan, in *Quark-Gluon Plasma 3*, edited by R. C. Hwa and Xin-Nian Wang (World Scientific, Singapore, 2004), pp. 249–3363; F. Gelis, E. Iancu, J. Jalilian-Marian, and R. Venugopalan, Annu. Rev. Nucl. Part. Sci. **60**, 463 (2010); F. Gelis, Int. J. Mod. Phys. E **24**, 1530008 (2015).

[2] L. D. McLerran and R. Venugopalan, Phys. Rev. D **49**, 2233 (1994); **49**, 3352 (1994); **50**, 2225 (1994).

[3] A. Kovner, L. D. McLerran, and H. Weigert, Phys. Rev. D **52**, 6231 (1995); **52**, 3809 (1995); I. Balitsky, Nucl. Phys. B **463**, 99 (1996); Y. V. Kovchegov, Phys. Rev. D **60**, 034008 (1999); E. Iancu, A. Leonidov, and L. D. McLerran, Nucl. Phys. A **692**, 583 (2001); Phys. Lett. B **510**, 133 (2001); E. Ferreiro, E. Iancu, A. Leonidov, and L. McLerran, Nucl. Phys. A **703**, 489 (2002); A. Dumitru and L. D. McLerran, *ibid.* **700**, 492 (2002); H. Weigert, Prog. Part. Nucl. Phys. **55**, 461 (2005).

[4] L. V. Gribov, E. M. Levin, and M. G. Ryskin, Phys. Rep. **100**, 1 (1983); A. H. Mueller and J.-W. Qiu, Nucl. Phys. B **268**, 427 (1986); J. P. Blaizot and A. H. Mueller, *ibid.* **289**, 847 (1987).

[5] V. Khachatryan *et al.* (CMS Collaboration), J. High Energy Phys. 09 (2010) 091.

[6] S. Chatrchyan *et al.* (CMS Collaboration), Phys. Lett. B **718**, 795 (2013).

[7] B. Abelev *et al.* (ALICE Collaboration), Phys. Lett. B **719**, 29 (2013).

[8] G. Aad *et al.* (ATLAS Collaboration), Phys. Rev. Lett. **110**, 182302 (2013).

[9] A. Adare *et al.* (PHENIX Collaboration), Phys. Rev. Lett. **111**, 212301 (2013).

[10] A. Adare *et al.* (PHENIX Collaboration), Phys. Rev. Lett. **114**, 192301 (2015).

[11] C. Aidala *et al.* (PHENIX Collaboration), Phys. Rev. Lett. **120**, 062302 (2018).

[12] C. Aidala *et al.* (PHENIX Collaboration), Nat. Phys. **15**, 214 (2019).

[13] K. Dusling, W. Li, and B. Schenke, Int. J. Mod. Phys. E **25**, 1630002 (2016).

[14] R. D. Weller and P. Romatschke, Phys. Lett. B **774**, 351 (2017).

[15] J. L. Nagle and W. A. Zajc, Annu. Rev. Nucl. Part. Sci. **68**, 211 (2018).

[16] C. Shen, U. Heinz, P. Huovinen, and H. Song, Phys. Rev. C **84**, 044903 (2011).

[17] P. Bozek, Phys. Rev. C **85**, 014911 (2012).

[18] Z. Qiu, C. Shen, and U. Heinz, Phys. Lett. B **707**, 151 (2012).

[19] Z. Qiu and U. Heinz, Phys. Rev. C **84**, 024911 (2011).

[20] B. Schenke, P. Tribedy, and R. Venugopalan, Phys. Rev. Lett. **108**, 252301 (2012).

[21] P. Bozek and I. Wyskiel-Piekarska, Phys. Rev. C **85**, 064915 (2012).

[22] C. Gale, S. Jeon, B. Schenke, P. Tribedy, and R. Venugopalan, Phys. Rev. Lett. **110**, 012302 (2013).

[23] Z. Qiu and U. Heinz, Phys. Lett. B **717**, 261 (2012).

[24] C. Gale, S. Jeon, and B. Schenke, Int. J. Mod. Phys. A **28**, 1340011 (2013).

[25] B. Schenke and R. Venugopalan, Phys. Rev. Lett. **113**, 102301 (2014).

[26] J. Noronha-Hostler, M. Luzum, and J. Y. Ollitrault, Phys. Rev. C **93**, 034912 (2016).

[27] S. Ryu, J.-F. Paquet, C. Shen, G. S. Denicol, B. Schenke, S. Jeon, and C. Gale, Phys. Rev. Lett. **115**, 132301 (2015).

[28] H. Niemi, K. J. Eskola, and R. Paatelainen, Phys. Rev. C **93**, 024907 (2016).

[29] C. Shen, Z. Qiu, and U. Heinz, Phys. Rev. C **92**, 014901 (2015).

[30] R. Derradi de Souza, T. Koide, and T. Kodama, Prog. Part. Nucl. Phys. **86**, 35 (2016).

[31] G. Giacalone, J. Noronha-Hostler, M. Luzum, and J. Y. Ollitrault, Phys. Rev. C **97**, 034904 (2018).

[32] T. Hirano, U. W. Heinz, D. Kharzeev, R. Lacey, and Y. Nara, Phys. Lett. B **636**, 299 (2006).

[33] T. Hirano, U. W. Heinz, D. Kharzeev, R. Lacey, and Y. Nara, J. Phys. G: Nucl. Part. Phys. **34**, S879 (2007).

[34] H. Song, S. A. Bass, U. Heinz, T. Hirano, and C. Shen, Phys. Rev. Lett. **106**, 192301 (2011); **109**, 139904(E) (2012).

[35] Z. Citron *et al.*, arXiv:1812.06772.

[36] Y. V. Kovchegov and K. Tuchin, Phys. Rev. D **65**, 074026 (2002).

[37] F. Gelis, T. Lappi, and R. Venugopalan, Phys. Rev. D **78**, 054019 (2008).

[38] J.-P. Blaizot, T. Lappi, and Y. Mehtar-Tani, Nucl. Phys. A **846**, 63 (2010).

[39] D. Kharzeev and E. Levin, Phys. Lett. B **523**, 79 (2001).

[40] A. Dumitru, D. E. Kharzeev, E. M. Levin, and Y. Nara, Phys. Rev. C **85**, 044920 (2012).

[41] E. Levin and A. H. Rezaeian, Phys. Rev. D **83**, 114001 (2011).

[42] P. Tribedy and R. Venugopalan, Phys. Lett. B **710**, 125 (2012); **718**, 1154(E) (2013).

[43] A. Dumitru, A. V. Giannini, M. Luzum, and Y. Nara, Phys. Lett. B **784**, 417 (2018).

[44] W. A. Horowitz and Y. V. Kovchegov, Nucl. Phys. A **849**, 72 (2011).

[45] J. L. Albacete, A. Dumitru, H. Fujii, and Y. Nara, Nucl. Phys. A **897**, 1 (2013).

[46] J. Cepila, J. G. Contreras, and M. Matas, Phys. Rev. D **99**, 051502(R) (2019).

[47] K. J. Golec-Biernat and A. M. Stasto, Nucl. Phys. B **668**, 345 (2003).

[48] Y. Kovchegov and H. Weigert, Nucl. Phys. A **784**, 188 (2007); I. I. Balitsky, Phys. Rev. D **75**, 014001 (2007); E. Gardi, J. Kuokkanen, K. Rummukainen, and H. Weigert, Nucl. Phys. A **784**, 282 (2007); I. Balitsky and G. A. Chirilli, Phys. Rev. D **77**, 014019 (2008).

[49] J. L. Albacete, N. Armesto, J. G. Milhano, and C. A. Salgado, Phys. Rev. D **80**, 034031 (2009).

[50] A. Dumitru, A. V. Giannini, M. Luzum, and Y. Nara, arXiv:1811.07696.

[51] Y. V. Kovchegov and H. Weigert, Nucl. Phys. A **807**, 158 (2008).

[52] Y. L. Dokshitzer, V. A. Khoze, and S. I. Troian, J. Phys. G: Nucl. Part. Phys. **17**, 1585 (1991).

[53] F. O. Durães, A. V. Giannini, V. P. Goncalves, and F. S. Navarra, Phys. Rev. D **94**, 054023 (2016).

[54] S. H. Lim, J. Carlson, C. Loizides, D. Lonardoni, J. E. Lynn, J. L. Nagle, J. D. Orjuela Koop, and J. Ouellette, Phys. Rev. C **99**, 044904 (2019).

[55] M. D. Sievert and J. Noronha-Hostler, arXiv:1901.01319.

[56] S. Huang, Z. Chen, J. Jia, and W. Li, arXiv:1904.10415.

[57] P. Huovinen and P. Petreczky, Nucl. Phys. A **837**, 26 (2010).

[58] J.-F. Paquet, C. Shen, G. S. Denicol, M. Luzum, B. Schenke, S. Jeon, and C. Gale, Phys. Rev. C **93**, 044906 (2016).

[59] B. Schenke, S. Jeon, and C. Gale, Phys. Rev. C **82**, 014903 (2010).

[60] S. A. Bass *et al.*, Prog. Part. Nucl. Phys. **41**, 255 (1998); M. Bleicher *et al.*, J. Phys. G: Nucl. Part. Phys. **25**, 1859 (1999).

[61] J. E. Bernhard, arXiv:1804.06469.

[62] C. Loizides, J. Nagle, and P. Steinberg, SoftwareX **1-2**, 13 (2015).

[63] S. S. Adler *et al.* (PHENIX Collaboration), Phys. Rev. C **71**, 034908(2005); **71**, 049901 (2005).
[64] B. B. Back *et al.* (PHOBOS Collaboration), Phys. Rev. C **65**, 061901 (2002).
[65] B. I. Abelev *et al.* (STAR Collaboration), Phys. Rev. C **79**, 034909 (2009).
[66] S. Chatrchyan *et al.* (CMS Collaboration), J. High Energy Phys. 08 (2011) 141.
[67] G. Aad *et al.* (ATLAS Collaboration), Phys. Lett. B **710**, 363 (2012).
[68] K. Aamodt *et al.* (ALICE Collaboration), Phys. Rev. Lett. **106**, 032301 (2011).
[69] S. Acharya *et al.* (ALICE Collaboration), Phys. Lett. B **790**, 35 (2019).
[70] B. B. Back *et al.* (PHOBOS Collaboration), Phys. Rev. Lett. **93**, 082301 (2004).
[71] B. Abelev *et al.* (ALICE Collaboration), Phys. Rev. Lett. **110**, 032301 (2013).
[72] A. M. Sirunyan *et al.* (CMS Collaboration), J. High Energy Phys. 01 (2018) 045.
[73] K. Dusling and R. Venugopalan, Phys. Rev. Lett. **108**, 262001 (2012).
[74] K. Dusling, M. Mace, and R. Venugopalan, Phys. Rev. D **97**, 016014 (2018).
[75] M. Mace, V. V. Skokov, P. Tribedy, and R. Venugopalan, Phys. Rev. Lett. **121**, 052301 (2018).
[76] S. S. Adler *et al.* (PHENIX Collaboration), Phys. Rev. C **69**, 034909 (2004).
[77] B. B. Abelev *et al.* (ALICE Collaboration), Phys. Lett. B **727**, 371 (2013).
[78] S. Acharya *et al.* (ALICE Collaboration), Phys. Lett. B **788**, 166 (2019).
[79] M. Gyulassy and T. Matsui, Phys. Rev. D **29**, 419 (1984).
[80] M. Gyulassy, Y. Pang, and B. Zhang, Nucl. Phys. A **626**, 999 (1997).
[81] A. Dumitru and M. Gyulassy, Phys. Lett. B **494**, 215 (2000).
[82] K. Aamodt *et al.* (ALICE Collaboration), Phys. Rev. Lett. **105**, 252302 (2010).
[83] K. Aamodt *et al.* (ALICE Collaboration), Phys. Rev. Lett. **107**, 032301 (2011).
[84] E. Retinskaya, M. Luzum, and J. Y. Ollitrault, Phys. Rev. C **89**, 014902 (2014).
[85] T. Hirano and Y. Nara, Phys. Rev. C **79**, 064904 (2009).
[86] T. Hirano, P. Huovinen, and Y. Nara, Phys. Rev. C **83**, 021902(R) (2011).
[87] T. Hirano, P. Huovinen, and Y. Nara, Phys. Rev. C **84**, 011901(R) (2011).